Journal of Organometallic Chemistry, 376 (1989) 419–439
Elsevier Sequoia S.A., Lausanne – Printed in The Netherlands
JOM 20098

New silyl-nickel complexes prepared by η^6-arene substitution in (η^6-toluene)bis(trihalosilyl)nickel. Preparation of $L_3Ni(SiX_3)_2$ and $L_2Ni(SiX_3)_2$ (X = Cl, F; L = phosphine, phosphites, and pyridines. X-Ray structure of *cis*-$(collidine)_2Ni(SiCl_3)_2$

Seok-Burm Choe, Joerg J. Schneider *, Kenneth J. Klabunde,
Department of Chemistry, Kansas State University, Manhattan, Kansas 66506 (U.S.A.)

Lewis J. Radonovich, and Thomas A. Ballintine
Department of Chemistry, University of North Dakota, Grand Forks, North Dakota 58202 (U.S.A.)

(Received May 1st, 1989)

Abstract

Facile displacement of the arene ligand in (η^6-toluene)$Ni(SiX_3)_2$ (X = F, Cl) has produced $L_2Ni(SiX_3)_2$ and $L_3Ni(SiX_3)_2$ complexes, where L = trimethylphosphine, triethylphosphine, trimethylphosphite, triethylphosphite, trifluorophosphine, pyridine, lutidine, or collidine. Steric factors appear to determine whether disubstituted (square planar) or trisubstituted (trigonal bipyramidal) systems are formed. In the case of the methyl-pyridine analogs the *cis*- and *trans*-$L_2Ni(SiCl_3)_2$ complexes can be differentiated by their NMR. These investigations have led to a wide range of new Ni–Si complexes, some of their chemical properties have been investigated, and an improved synthesis of (η^6-toluene)$Ni(SiF_3)_2$ is reported. An X-ray structure determination of $Ni(SiCl_3)_2((CH_3)_3C_5H_2N)_2$ reveals that a distorted square planar geometry exists in the solid state with equivalent ligands in a *cis*-configuration. The complex crystallizes in space group $P2_1/c$ with lattice constants of *a* 8.964(5), *b* 15.0591(9), *c* 18.273(1) Å, and β 86.689(2)°. The steric bulk of the collidine ligand is accommodated by a ~ 28° rotation of the NiN_2 plane relative to the $NiSi_2$ plane which is closer to square planar (0°) than tetrahedral (90°). An analysis of bond parameters indicates that some π-backbonding to the $SiCl_3$ groups exists which helps to stabilize the complex.

---

* Current address: Max Planck Institut für Kohlenforschung, 4330 Mülheim a.d. Ruhr (West Germany).

0022-328X/89/$03.50

Introduction

The possibility of forming bonds between transition metals and the lower group 14 elements (Si, Ge, Sn, Pb) was recognized as early as 1941 by Hein and coworkers dealing with Fe–Pb complexes [1]. However, it was not until 1956 that the first transition metal silyl complex, $CpFe(CO)_2Si(CH_3)_3$, was reported [2]. Ten more years passed before other transition metal silyl complexes were reported [3,4]. Since that time many such silyl complexes have been reported and now most transition metals are known to form bonds with silicon. For the nickel triad most work has been concerned with Pt due to the interest in hydrosilation catalysts. The few silylnickel complexes that have been reported [5–14] generally have been prepared by oxidative addition of Si–Si [7,10], Si–R [8,9,11,13], and Si–H [5,9] bonds to Ni^0 complexes although some have been prepared by ligand exchange at the Ni center [11,12].

Ligated nickelsilylhalides possess three unique active bonds:

$$\mathrm{L} \overset{a}{-} \mathrm{Ni} \overset{b}{-} \mathrm{Si} \overset{c}{-} \mathrm{X}$$

The ligand–nickel bond (a), is the main concern of this study. Glocking and coworkers [5,6] have reported exchange of $SiCl_3$ for $GeCl_3$, at site (b) and Kiso and coworkers [13] have reported diphenylacetylene insertion into Ni–Si bonds. Site (c) is also of interest but little studied. There is one report of halide-ethyl exchange using Et_4Pb or Et_2Hg as an alkylating agent [6]. We are reporting one very useful reaction at site (c), the conversion of $SiCl_3$ groups to SiF_3 groups with $AgBF_4$.

Our recent discovery of a good synthetic entry into L–Ni–Si–X complexes where L = arene (**1**) [15,16], and the fact that the arene is extremely labile, provided us with starting materials for catalytic studies [17a] as well as preparation of new L–Ni–Si–X systems. Initial studies led to a new carbonyl complex as reported previously [17b]. The question of how many neutral ligands the $Ni(SiCl_3)_2$ moiety will accommodate led us to pursue the following investigations [18]. Moreover, an X-ray structure determination of one type **3** complex (where X = Cl and L = $(CH_3)_3C_5H_2N$) was carried out in order to provide a direct comparison to the previously reported type **2** complex.

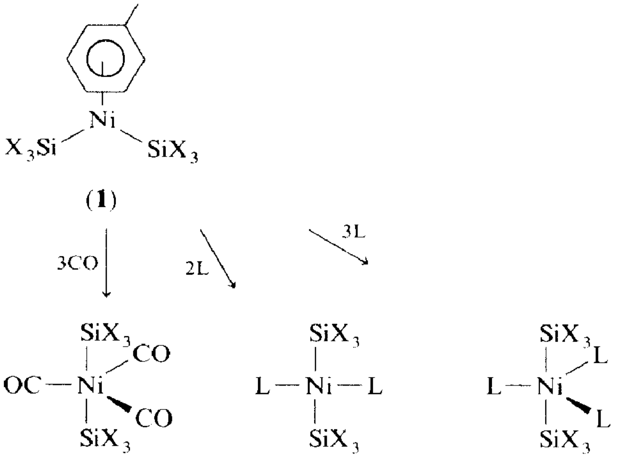

(**1**)

(**2**, X = Cl) (**3**, X = F or Cl) (**4**, X = F or Cl)

Results and discussion

Formation of 3 or 4

Complex **1** is an 18-electron system, and one might expect that three neutral (two electron donor) ligands would add to the nickel upon arene displacement. However, the most common nickel(II) compounds are square planar L_2NiR_2 16-electron systems [19]. The geometry about the nickel center is explainable by a combination of ligand field and steric effects. In order to probe these factors (keeping in mind our findings when **2** was prepared) [17b], we examined the products formed using a series of ligands and determined which ligands produced complexes of stoichiometry **3** or **4**. This series of interesting new compounds is shown below in Scheme 1.

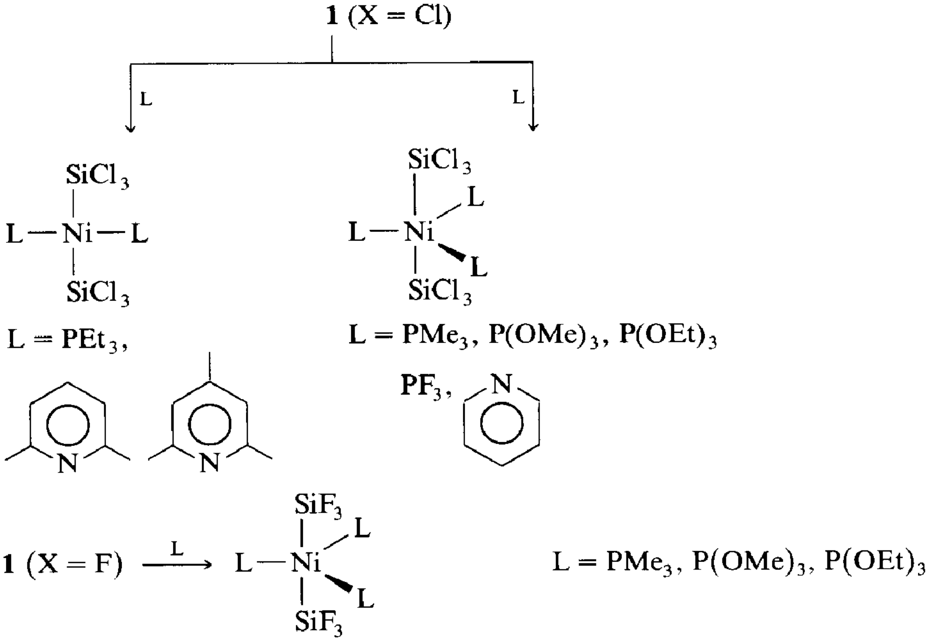

Scheme 1

In the case of phosphorus ligands, steric effects, as expressed by cone angle, explain our results nicely [20]. Thus, $P(OMe)_3$, $P(OEt)_3$, PMe_3, and PF_3 with cone angles of less than 120° yield trisubstituted products, while PEt_3 with a cone angle greater than 120°, yields only the disubstituted product.

In the case of the nitrogen ligands, steric effects are also important. Comparison of pyridine with the methyl substituted analogs shows that methyl substitution at the 2,6-positions causes a shift from stoichiometry 4 to 3.

Structures of complexes

A. Phosphorus ligands. For stoichiometry **4** where L = PMe_3, $P(OMe)_3$, $P(OEt)_3$, and PF_3 there are two idealized geometries that are possible; the trigonal bipyramid and the square base pyramid (Fig. 1). The ^{31}P NMR spectra of these complexes indicate only one environment for phosphorus, and when SiF_3 is present splitting of the ^{31}P resonance by six equivalent fluorines is observed (see Table 1 for NMR data). Of the six possible isomers, only (d) of Fig. 1 fits these NMR data if one assumes that rapid ligand exchange does not occur. Further support is provided by the X-ray structural determination of **2** [17b] which has this geometry. Thus, it is likely that the complexes reported herein are analogs of **2** and have this symmetrical trigonal bipyramidal structure represented by (d) of Fig. 1.

For compounds of stoichiometry **3** two limiting geometries are possible for the idealized coordination sphere; square planar (D_{4h}) and tetrahedral (T_d). In general, Ni^{2+} is expected to form square planar complexes with strongly complexing ligands when steric effects are not serious. Although it is difficult to differentiate these two possibilities for $(Et_3P)_2Ni(SiCl_3)_2$, tetrahedral complexes are expected to be paramagnetic [21*], while square planar complexes are diamagnetic. Since the complex is not paramagnetic we conclude that a square planar geometry provides the best fit of the data. This is further supported by the observed results for the substituted pyridine complexes discussed in the next section.

B. Nitrogen ligands. Pyridine and substituted pyridines were investigated as ligands because these heteroaromatics have the potential to bind in a σ- or π-fashion to the metal. Although π-bonded heteroaromatic complexes of the early transition metals are known [22*] no analogous late transition metal systems have been reported. For the late transition metals σ-bond formation is most favorable and a large number of such compounds are known [23,24], including a few pyridine and substituted pyridine complexes [25,26].

The (η^6-arene)$Ni(SiX_3)_2$ system seems to be uniquely suited for possibly obtaining a π-pyridine complex. However, our results show that even with the sterically hindered methyl substituted pyridines (2,6-lutidine and 2,4,6-collidine), only σ-complexes are formed.

The role of steric factors is demonstrated by considering the type of complex that is formed with a variety of pyridines. When severe steric restrictions are present, as with 2,6-di-t-butylpyridine no reaction occurs, when moderate steric restrictions are present, as with 2,6-butidine and 2,4,6-collidine, $L_2Ni(SiX_3)_2$ systems are formed. For unsubstituted pyridine $L_3Ni(SiX_3)$ is produced (compounds **5**, **6** and **7**).

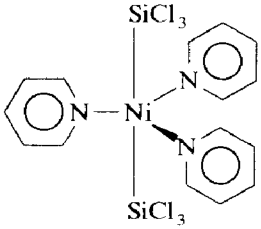

(5)

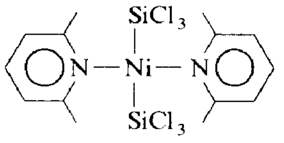

(6)

(2,6-lutidine = L)

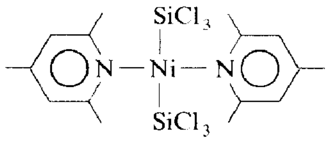

(7)

(2,4,6-collidine = L)

These materials are very air sensitive, and in solution (with air) deep green-blue solutions form in seconds with release of some of the pyridine ligands. Products **5**, **6**, and **7** are insoluble in toluene, ether, and pentane. Solubility in $CHCl_3$ and CH_2Cl_2 is in the order **6** > **7** > **5** > .

It is somewhat surprising that the methyl substituted pyridines do not yield π-complexes based on prior reports [27], in particular noting earlier metal atom reactions [27a–27e]. Apparently in our case, the reaction partners are able to react much more according to chemical preference (thermodynamic control rather than

---

* Reference numbers with asterisks indicate notes in the list of references.

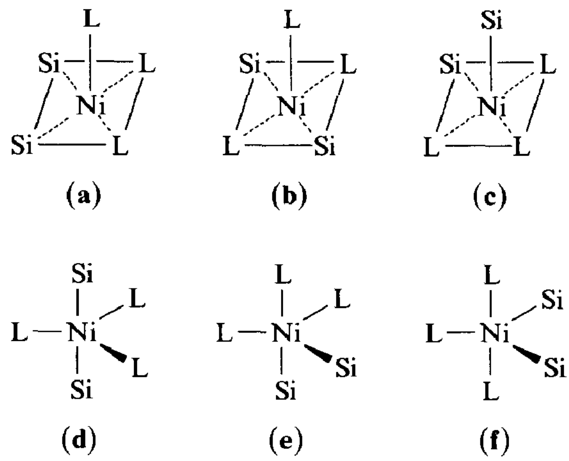

Fig. 1. Possible structural isomers for $L_3Ni(SiX_3)_2$.

kinetic control), and the steric hindrance of the σ-bonding site is not enough to prevent σ-bonding in favor of π-bonding.

The first complex of square planar nickel(II) with a neutral monodentate amine was reported in 1978 [28]. Neither that report nor more recent ones [29] indicate *cis/trans* isomers for these square planar complexes. In **6** and **7**, however, we believe *cis*- and *trans*-isomers are formed and are differentiable by NMR (Fig. 2). First, this observation requires that the overall structures be square planar rather than tetrahedral. Second, it requires that **6** and **7** are not highly labile.

The NMR data shows that the two isomers are present in different ratios (1/3 for **6** and 1/4 for **7**). The *trans*-isomer might be expected to be the favored one.

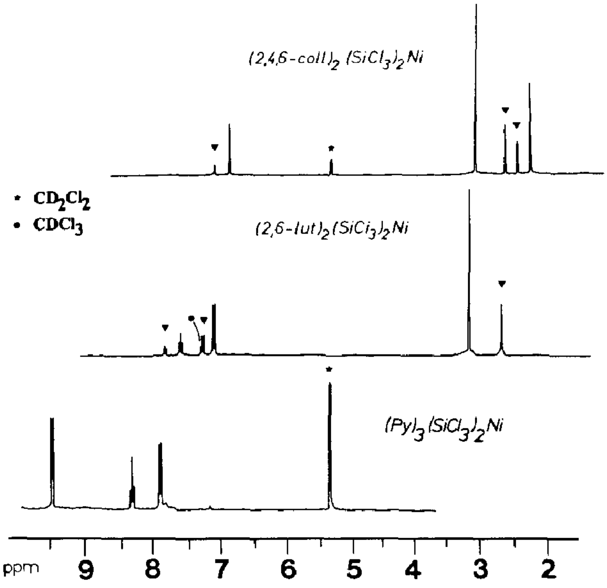

Fig. 2. ^1H NMR spectra for $(lutidine)_2Ni(SiCl_3)_2$ and $(collidine)_2Ni(SiCl_3)_2$. Solid triangles denote the *trans*-isomer absorptions.

Table 1

NMR data for complexes prepared

Compound	^{1}H $CDCl_3$ solv. (ppm. TMS std.)	^{31}P ($CDCl_3$ solv)	^{19}F ppm. C_6F_6 std.	^{13}C
(η^6-Toluene)Ni$(SiCl_3)_2$	2.65(s), CH_3 6.75(m), C_6H_5			
(η^6-Toluene)Ni$(SiF_3)_2$	2.50(s), CH_3 6.80(m), C_6H_5		74.0 singlet (downfield from C_6F_6, in CD_2Cl_2) J(F–Si) 189 Hz	
$(Me_3P)_3Ni(SiCl_3)_2$	1.80 (4 peaks with 2 Hz spacing) [a]	–173.05 singlet $(MeO)_3P$ std.)		
$(Me_3P)_3Ni(SiF_3)_2$	1.50 (4 peaks with 2 Hz spacing) [a]	–163.6 septet J(P–F) 5.8 Hz ($(MeO)_3P$ std.)		
$[(MeO)_3P]_3Ni(SiCl_3)_2$	3.83 (4 peaks with 4 Hz spacing) [a]			
$[(MeO)_3P]_3Ni(SiF_3)_2$	3.68 (4 peaks with 4 Hz spacing) [a]	–11.3 septet J(P–F) 5.2 Hz ($(MeO)_3P$ std.)		
$[(EtO)_3P]_3Ni(SiCl_3)_2$	1.40 triplet 4.25 multiplet			
$[(EtO)_3P]_3Ni(SiF_3)_2$	1.30 triplet 4.02 multiplet	–6.22 septet J(P–F) 5.8 Hz ($(MeO)_3P$ std.)		
$(Et_3P)_2Ni(SiCl_3)_2$	1.33 triplet 1.67 multiplet			
$(Lutidine)_2Ni(SiCl_3)_2$ [b]	*cis* 3.16 singlet (CH_3) 7.04 doublet (*m*-H) (in $CDCl_3$) 7.58 triplet (*p*-H) *trans* 2.76 singlet (CH_3) 7.32 doublet (*m*-H) 7.88 triplet (*p*-H)			
$(Collidine)_2Ni(SiCl_3)_2$ [c]	*cis* 3.09 singlet (2,6-CH_3) (in CD_2Cl_2) (*m*-H) 2.25 singlet (4-CH_3) *trans* 2.68 singlet (2,6-CH_3) 7.18 singlet (*m*-H) 2.47 singlet (4-CH_3)			

Table 1 (continued)

Compound	^{1}H CDCl$_3$ solv. (ppm. TMS std.)	^{31}P (CDCl$_3$ solv)	^{19}F ppm. C_6F_6 std.	^{13}C
$(Pyridine)_3Ni(SiCl_3)_2$ [d]	9.45 doublet (*o*-H) (in CD_2Cl_2) 7.84 doublet (*m*-H) 8.35 triplet (*p*-H)			
$[(MeO)_3P]_2$ $Ni(SiCl_3)_2(CO)$	3.30 triplet *J*(H–P) 5.0 Hz	−121.77 (in C_6H_6, H_3PO_4 ext.std.)		CO 188.53 triplet $J(^{13}C–P)$ 54.0 Hz CH_3 52.8 singlet
$(F_3P)_3Ni(SiCl_3)_2$		see Table 3	21.90 doublet *J*(P–F) 1.445 Hz (in $CDCl_3$, $CFCl_3$ std.)	

[a] These are distorted quartets due to AA′A″X configuration. [b] The free ligand 2,6-lutidine has absorptions at 2.52 (CH_3), 6.95 (*m*-H), and 7.46 (*p*-H). [c] The free ligand 2,4,6-collidine has absorptions at 2.44 (2,6-CH_3), 6.77 (*m*-H), and 2.30 (4-CH_3). [d] The free ligand pyridine has absorptions at 8.51 (*o*-H), 7.18 (*m*-H), and 7.56 (*p*-H).

However, a single crystal X-ray structural analysis of **7** indicated a distorted *cis*-configuration (see later discussion). We did not observe different crystal habits in the solid, and therefore suspect that the *cis* is the favored isomer. Thus, we tentatively assign the NMR spectrum of the *cis* to the predominant isomer, and it may be that the paramagnetic anisotropy of the Ni atom causes the deshielding of the *ortho*-CH_3 protons in the *cis* more than the *trans* [30]. However, until further work yields structural and NMR parameters for the *trans* as well as the *cis*, we cannot be sure.

IR data for **6** and **7** may also support the formation of *cis*/*trans* isomers. It is known that the out-of-plane vibrations in methyl-substituted pyridines are very sensitive to the geometry of corresponding nickel(II), palladium(II), and platinum(II) complexes [31]. For 2,6-lutidine and 2,4,6-collidine these medium to strong bands appear in the 750–850 cm^{-1} region. For their complexes **6** and **7** the bands are split, which could be explained by the existence of two isomers (Fig. 3). It should be noted that such splitting is not observed in pure *trans*-isomers, for example with copper(II) complexes [32]. As pointed out by a reviewer, however, these splittings also may be due to slightly different environments of the methyl groups within the same isomer (see discussion of X-ray structure below). We cannot differentiate these two possibilities at this time.

As mentioned above, we were able to structurally analyze one of the isomers, which turned out to be the *cis*-configuration of **7**. Thus, an ORTEP diagram of one molecule of $Ni(SiCl_3)_2((CH_3)_3C_5H_2N)_2$ as it exists in the solid state is shown in Fig. 4. The nickel atom is σ-bonded to two nitrogen atoms from 2,4,6-collidine

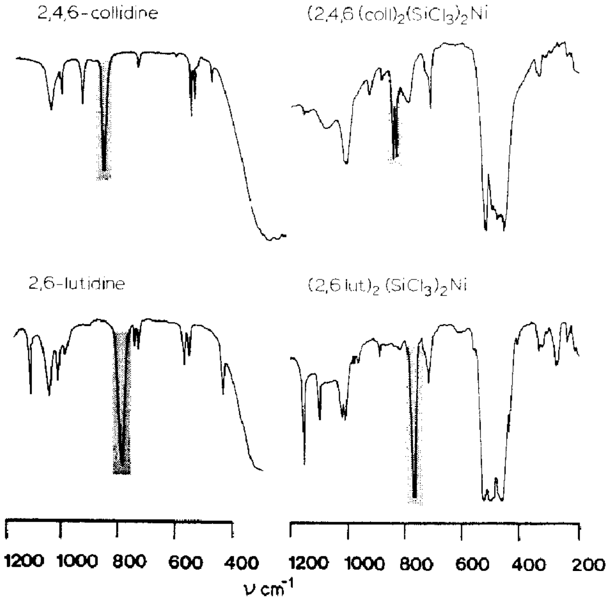

Fig. 3. IR spectra for $(\text{lutidine})_2\text{Ni}(\text{SiCl}_3)_2$ and $(\text{collidine})_2\text{Ni}(\text{SiCl}_3)_2$.

ligands and two SiCl_3 groups. Bond distances and angles are listed in Tables 2 to 5. The geometry of the coordination sphere is distorted square planar with equivalent donor atoms in a *cis*-configuration. Individual deviations from the mean plane

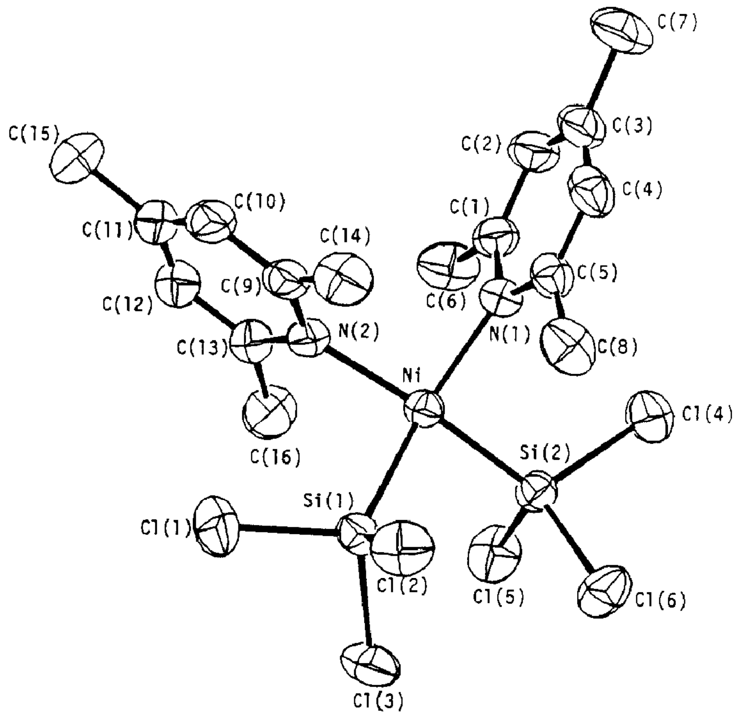

Fig. 4. An ORTEP diagram of $\text{Ni}(\text{SiCl}_3)_2(\text{CH}_3)_3\text{C}_5\text{H}_2\text{N})_2$ as it exists in the crystal. Hydrogen atoms have been omitted for clarity.

Table 2

Bond distances (Å) in $Ni(SiCl_3)_2((CH_3)_3C_5H_2N)_2$

Ni–N(01)	1.987(3)
Ni–N(02)	2.000(3)
Ni–Si(02)	2.195(1)
Ni–Si(01)	2.208(1)
C(01)–N(01)	1.356(4)
C(01)–C(02)	1.384(5)
C(01)–C(06)	1.481(5)
C(02)–C(03)	1.392(6)
C(03)–C(04)	1.372(6)
C(03)–C(07)	1.519(5)
C(04)–C(05)	1.378(5)
C(05)–N(01)	1.351(4)
C(05)–C(08)	1.506(5)
C(09)–N(02)	1.356(4)
C(09)–C(10)	1.398(5)
C(09)–C(14)	1.492(6)
C(10)–C(11)	1.370(6)
C(11)–C(12)	1.367(6)
C(11)–C(15)	1.503(6)
C(12)–C(13)	1.380(5)
C(13)–N(02)	1.360(5)
C(13)–C(16)	1.506(5)
Si(01)–Cl(01)	2.079(1)
Si(01)–Cl(02)	2.087(1)
Si(01)–Cl(03)	2.069(1)
Si(02)–Cl(04)	2.083(1)
Si(02)–Cl(05)	2.073(1)
Si(02)–Cl(06)	2.071(1)

containing Ni,N(01),N(02),Si(01), and Si(02) are 0.004, 0.38, −0.37, 0.34, and −0.35 Å, respectively. The magnitude of the distortion from square planar geometry can also be expressed in terms of a dihedral rotation angle between the plane defined by Ni,Si(01),Si(02) and the plane defined by Ni,N(01),N(02). A value of 27.9° is observed for the complex which is consideraly closer to the square planar angle of 0° than the tetrahedral angle 90°. Thus the coordination sphere displays a significant distortion from a planar geometry but is still much closer to square planar than tetrahedral.

An important factor that favors square planar over tetrahedral geometry is the capability of π-back bonding to the ligands. The extent of π-back bonding would be expected to affect the Ni–ligand bond distances. In particular, the $Ni–SiCl_3$ distance could serve as a convenient probe because several structure determinations of nickel complexes have recently been carried out [17b,33]. As the $Ni–SiCl_3$ π-back bonding increases the Ni–Si distances should decrease because of the higher bond order while the Si–Cl distances should increase due to the population of the π^* orbitals of $SiCl_3$. Listed in Table 4 are the average values for $Ni–SiCl_3$ bonds and Si–Cl bonds in the three structures. In $Ni(SiCl_3)_2(CO)_3$ the two $SiCl_3$ ligands occupy axial sites and function as good σ-donors [17b]. Thus, the $Ni–SiCl_3$ length of 2.286(3) Å should represent the case of little or no π-back bonding. In the dimeric anion $[Ni(SiCl_3)_2Cl_2]_2^{2-}$ the nickel coordination sphere is square planar

Table 3

Bond angles (deg) in $Ni(SiCl_3)_2((CH_3)_3C_5H_2N)_2$

N(01)–Ni–N(02)	92.41(11)
N(01)–Ni–Si(02)	91.66(8)
N(01)–Ni–Si(01)	160.35(8)
N(02)–Ni–Si(02)	159.96(9)
N(02)–Ni–Si(01)	93.01(8)
Si(02)–Ni–Si(01)	89.68(4)
N(01)–C(01)–C(02)	120.91(34)
N(01)–C(01)–C(06)	118.09(30)
C(02)–C(01)–C(06)	120.99(33)
C(01)–C(02)–C(03)	120.69(36)
C(04)–C(03)–C(02)	117.13(33)
C(04)–C(03)–C(07)	122.54(42)
C(02)–C(03)–C(07)	120.32(42)
C(03)–C(04)–C(05)	120.75(36)
N(01)–C(05)–C(04)	121.79(34)
N(01)–C(05)–C(08)	117.92(30)
C(04)–C(05)–C(08)	120.26(33)
N(02)–C(09)–C(10)	120.70(37)
N(02)–C(09)–C(14)	118.38(33)
C(10)–C(09)–C(14)	120.92(36)
C(11)–C(10)–C(09)	121.42(38)
C(12)–C(11)–C(10)	116.79(37)
C(12)–C(11)–C(15)	122.23(47)
C(10)–C(11)–C(15)	120.98(44)
C(11)–C(12)–C(13)	121.63(42)
N(02)–C(13)–C(12)	121.35(37)
N(02)–C(13)–C(16)	118.90(31)
C(12)–C(13)–C(16)	119.75(37)
C(05)–N(01)–C(01)	118.40(28)
C(05)–N(01)–Ni	118.66(22)
C(01)–N(01)–Ni	122.47(22)
C(09)–N(02)–C(13)	117.95(31)
C(09)–N(02)–Ni	124.13(25)
C(13)–N(02)–Ni	117.54(23)
Cl(03)–Si(01)–Cl(01)	100.80(6)
Cl(03)–Si(01)–Cl(02)	102.89(6)
Cl(03)–Si(01)–Ni	126.90(6)
Cl(01)–Si(01)–Cl(02)	101.30(7)
Cl(01)–Si(01)–Ni	115.43(6)
Cl(02)–Si(01)–Ni	106.22(5)
Cl(06)–Si(02)–Cl(05)	105.74(6)
Cl(06)–Si(02)–Cl(04)	99.07(6)
Cl(06)–Si(02)–Ni	124.11(5)
Cl(05)–Si(02)–Cl(04)	101.15(6)
Cl(05)–Si(02)–Ni	109.23(5)
Cl(04)–Si(02)–Ni	114.83(5)

and the Ni–$SiCl_3$ length is reduced to 2.171(3) Å indicating a considerable amount of π-back bonding [33]. In the present case the Ni–$SiCl_3$ length indicates some π-back bonding but slightly less than that in $[Ni(SiCl_3)_2Cl]_2^{2-}$. Comparison of the Si–Cl bond length is inherently more difficult because the Cl atoms are terminal and the value observed in an X-ray structure determination is affected by the size of

Table 4

Comparison of Ni-$SiCl_3$ bond parameters

	$Ni(SiCl_3)_2(CO)_3$	$[Ni(SiCl_3)_2Cl_2]_2^{2-}$	$Ni(SiCl_3)_2((CH_3)_3C_5H_2N)_2$
Ni–$SiCl_3$	2.286(3)	2.171(3)	2.202(1)
Si–Cl	2.032(5)	2.066(4)	2.077(1)
Si–Cl(Corr) [a]		2.096(4)	2.096(1)

[a] The average Si–Cl bond length after correcting for thermal motion [34] assuming the Cl atoms ride the Si atoms.

the thermal parameters. As the thermal parameters get large the apparent Si–Cl bond length will be reduced. Based upon the Ni–Si lengths one would expect a slightly larger value of the Si–Cl length in $[NiSiCl_3)_2Cl_2^{2-}$ which is not the case ignoring thermal motion. However, the average Cl thermal parameter in $[Ni(SiCl_3)_2Cl_2]^{2-}$ is ~ 30% larger than that observed in the present work. When the Si–Cl bond lengths are corrected for the effects of thermal motion [34], an identical Si–Cl of 2.906 Å distance is obtained. Most importantly, both structures that have

Table 5

Crystal data for $Ni(SiCl_3)_2((CH_3)_3C_5H_2N)_2$

formula:	$NiC_{16}H_{22}N_2Si_2Cl_6$
formula weight, amu:	569.97
space group:	$P2_1/c$
systematic absences:	$h\ 0\ l\ (l = 2n+1)$ $0\ k\ 0\ (k = 2n+1)$
a, Å	8.964(5)
b, Å	15.0591(9)
c, Å	18.273(1)
β, deg	86.698(2)
Z	4
density, calc, g/ml, at 23° C	1.54
crystal size, mm:	0.27 × 0.40 × 0.43
data collcn instrum:	Picker/CRYSTAL LOGIC
orientation reflections:	
no.; range, deg:	39; $9.8 \leq 2\theta \leq 20.4$
temp., ° C:	26
scan type:	2θ
data collection limits, deg:	$2 \leq 2\theta \leq 50.67$
data collected:	$h, k, \pm l$
no. unique data collected:	4478
data observed ($I > 3\sigma_I$):	3179
number of parameters refined:	244
u (Mo-K_α), mm^{-1}:	1.55
range of absorption factors:	0.739–0.808
weighting scheme:	$1/\sigma^2$
R	3.1%
R_w	4.2%
GOF	1.52
data/parameter ratio:	13
largest residual peak, $e^-/Å^3$:	1.52

Table 6

IR spectral data for various substituted carbonyl complexes

Compound	ν(C=O) (cm^{-1})	Reference
$[(MeO)_3P]_2Ni(SiCl_3)_2(CO)$	2060s, 1995w	this work
$(Me_3P)_2NiCl_2(CO)$	2005s, 1960w, 1955w	36
$(Me_3P)_2NiBr_2(CO)$	2010s, 1965w	36
$(Me_3P)_2NiI_2(CO)$	2015s, 2057s	36
$Ni(CO)_4$	2057s	37

significant π-back bonding display an increase in the Si–Cl bond length compared to $Ni(SiCl_3)_2(CO)_3$. Accordingly, this suggests that a significant amount of π-back bonding occurs in $Ni(SiCl_3)_2((CH_3)_3C_5H_2N)_2$, but the distortion from square planar geometry probably reduces the π-back bonding slightly.

The six-membered rings of the 2,4,6-collidine ligands are reasonably planar. The ligand containing N(01) has an average deviation of 0.02 Å while the ring containing N(02) has an average deviation of 0.01 Å. In both rings the N atom displays the largest out of plane displacement of 0.035 Å for N(01) and 0.024 Å for N(02) in their respective rings. In both rings the methyl groups show small displacements from the ring planes amounting to an average displacement of 0.11 and 0.07 Å for the rings containing N(01) and N(02) respectively.

In summary, the results of this structure determination reflect the strong tendency of Ni^{2+} to form square planar complexes with ligands that have π-back bonding capacity. Steric effects due to the bulky methyl substituents are alleviated by a ~ 28° rotation of the $NiSi_2$ plane relative to the NiN_2 plane thus reducing the nonbonded repulsions between methyl hydrogens from collidine and chlorine atoms from the $SiCl_3$ ligands. Apparently this rotation still allows a significant amount of π-back bonding to the $SiCl_3$ groups which helps to stabilize the complex.

Our conclusions then regarding structure for these pyridine compounds are that: (1) pyridine itself gives an $L_3Ni(SiCl_3)_2$ trigonal bipyramidal structure with pyridine rings pointing out in a propeller fashion; (2) the methyl-substituted pyridines yield $L_2Ni(SiCl_3)_2$ complexes with distorted square planar geometries. An unusual

Table 7

IR absorptions and ^{31}P chemical shifts of PF_3 complexes

Compound	IR ν(P–F) (cm^{-1})	^{31}P NMR (ppm, H_3PO_4 ext. std.)	Reference
$(F_3P)_3Ni(SiCl_3)_2$	920s, 910s	− 116.5 quartet J(P–F) 1.377 Hz (in $C_6H_5CF_3$)	this work
$Ni(PF_3)_4$	904s, 864s	− 127.5 quartet J(P–F) 1.300 Hz	39
PF_3	892s, 848s	− 97 quartet J(P–F) 1,410 Hz	39

feature is that spectral analyses indicate the formation of observable *cis*- and *trans*-isomers in the cases of **6** and **7**.

Some chemical investigations of $[(MeO)_3P]_3Ni(SiCl_3)_2$ and $(F_3P)_3Ni(SiCl_3)_2$ and the attempted preparation of $(F_3P)_3Ni(SiF_3)_2$

In order to learn more about the nature of these $L_3Ni(SiX_3)_2$ derivatives, some reaction studies have been carried out.

First, an attempt to form a Ni–Si–Co derivative was carried out according to Scheme 2. We anticipated that **8** would be formed by the well established "alkali salt elimination" route [35–37]. Instead, the substitution product **9** was formed along with the well known cobalt carbonyl complex **10**.

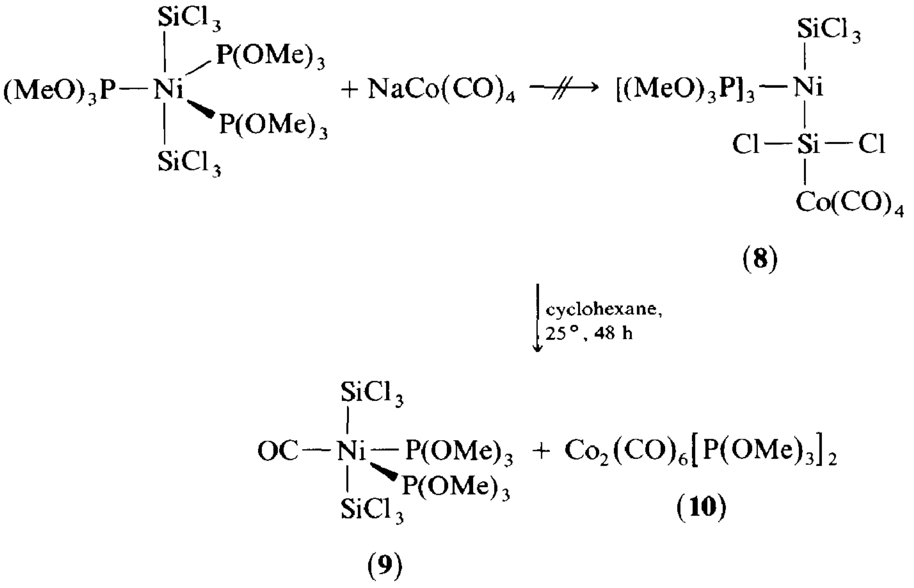

Scheme 2

Compound **9** is interesting in its own right. A relatively weak Ni–CO bond is apparent, which may explain why only one CO ligand is taken up. Comparison of the IR stretching frequencies for monosubstituted CO compounds (Table 6) shows that equatorial ligands which show no π-acceptor ability, such as Cl, Br, result in stronger Ni–C bonds and weaker C≡O bonds (e.g. the shortest Ni–CO bond length of 1.73 Å is found in $I_2(PMe_3)NiCO$) [38]. However, compound **9**, which is rich in π-acceptor ligands, exhibits a relatively high $\nu(C=O)$ frequency consistent with the fact that CO must compete with the other ligands for π-electron density (*trans* ligands compete for electron density from the same orbitals on the metal (d_{xy}, $d_{x^2-y^2}$) [38,39].

Our success in preparing the volatile, labile complex $(OC)_3Ni(SiCl_3)_2$ (**2**) [17b] encouraged us to prepare PF_3 analogs. The reaction of (η^6-toluene)$Ni(SiCl_3)_2$ with PF_3 proceeded nicely to yield $(F_3P)_3Ni(SiCl_3)_2$ (**11**). Compound **11** is more stable than **2**, can be exposed to air for short periods and can be sublimed at 35 °C under vacuum with no decomposition. IR studies of **11** show $\nu(P–F)$ at relatively high frequencies suggesting a weak Ni–P bond. This is reasonable considering that three equatorial PF_3 groups are competing for electron density from the same metal orbitals, and corresponds with experimental observations for many known PF_3 complexes (See Table 7) [40,41]. Such weak Ni–P bonds would suggest a modicum of lability for **11**, and we found that **11** could be converted back to **1** (X = Cl) by heating to 80 °C with excess toluene in $CDCl_3$ (sealed NMR tube). Thus, as with **2**, a reversible reaction is possible that depends on reaction conditions. The conversion of **1** to **11** is best carried out by treating solid **1** with PF_3 gas. The reverse reaction works best when pure **11** is treated with a high excess of arene and heat:

$$\underset{(X = Cl)}{\mathbf{1}} \underset{\text{toluene excess, } 80\,^{\circ}C}{\overset{PF_3 \text{ excess, } 25\,^{\circ}C}{\rightleftharpoons}} \mathbf{11}$$

In order to prepare perchloro and perfluoro derivatives of **11**, reactions of **1** (X = Cl or F) shown below were attempted. Unfortunately these were not successful. We assume that steric effects take precedence in the attempted preparation of **12**, and for both **12** and **13** the competition for electron density among the various electron demanding ligands causes the observed results. (Actually, the attempted preparation of **12** yielded a product at −20 °C, which actually may be **12**, but which decomposed upon workup).

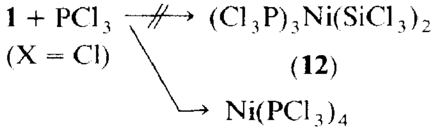

$$\begin{array}{lll} \mathbf{1} + PCl_3 & \not\longrightarrow & (Cl_3P)_3Ni(SiCl_3)_2 \\ (X = Cl) & & (\mathbf{12}) \\ & \searrow & Ni(PCl_3)_4 \end{array}$$

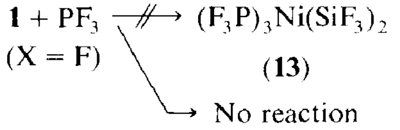

$$\begin{array}{lll} \mathbf{1} + PF_3 & \not\longrightarrow & (F_3P)_3Ni(SiF_3)_2 \\ (X = F) & & (\mathbf{13}) \\ & \searrow & \text{No reaction} \end{array}$$

Fluorination of $Ni(SiCl_3)_2$ to $Ni(SiF_3)_2$

The preparation of the $(\eta^6\text{-arene})Ni(SiCl_3)_2$ derivatives employs the reaction of $(allyl)_2Ni$ derivatives with $HSiCl_3$ in the presence of an appropriate arene. This reaction works very well and large amounts of **1** are now available.

In order to prepare $(\eta^6\text{-arene})Ni(SiF_3)_2$ the same reaction sequence using $HSiF_3$ can be used [16,18,42]. However, $HSiF_3$ is a difficult material to obtain pure and we sought a more convenient synthetic route. In the conversion of the Si–Cl to SiF thermodynamics would be greatly in our favor [43]. However, converting the $Ni(SiCl_3)_2$ to $Ni(SiF_3)_2$ seemed an unlikely possibility since we thought the Ni–Si bond would be too sensitive to fluorinating agents. However, this direct conversion can indeed be carried out smoothly with $AgBF_4$, a rather mild fluorinating agent. This is an important discovery and should be quite useful in the preparation of a variety of M-SiF_3 derivatives.

$$\underset{(X = Cl)}{\mathbf{1}} + 6AgBF_4 \longrightarrow \underset{(X = F)}{\mathbf{1}} + 6AgCl + 6BF_3$$

Experimental

Chemicals were purified as follows: PMe_3, PEt_3, $P(OMe)_3$ and $P(OEt)_3$ were degassed and used as received (Aldrich or Organomet., Inc.,); $HSiCl_3$ (Aldrich) was freed of dissolved HCl by treating in vacuum at −78° C for one hour; 2,6-lutidine and 2,4,6-collidine (Aldrich, 99%) were used as received; pyridine was dried over KOH pellets and distilled from BaO prior to use; $NiCl_2 \cdot 6H_2O$ (Aldrich) was dehydrated at 160° C for several weeks prior to use; PF_3 (Ozark–Mahoning 99.9%) was used as received; $NaCo(CO)_4$ was prepared from $Co_2(CO)_8$ (Alfa Products) according to the method of Edgell and Lyford [44]. BF_3 (Matheson) was used as received; Ag_2O (Fisher) was placed under vacuum several hours prior to use; BCl_3 (Aldrich, research grade) and $C_6H_5CF_3$ (Aldrich gold label) were used as received. Solvents (diethyl ether, pentane, toluene) were continuously refluxed over sodium benzophenone ketyl under prepurified N_2 or Na/K alloy (THF) and distilled prior to use; cyclohexane (Aldrich, spectrometric grade) was used as received.

Manipulations of solids and solutions were carried out either in Schlenk airless apparatus under argon or in an argon filled glove box (Vacuum Atmospheres Dri-Lab with He-493 Dri-Train).

Physical measurements were carried out using: IR, Perkin–Elmer IR 1330; NMR, Bruker WM 400 FT-NMR for ^1H at 400.1 MHz, for ^{31}P at 162.0 MHz, for ^{19}F at 376.5 MHz, for ^{13}C at 100.6 MHz. Mass spectra were obtained on a Finnigan Quadrupole instrument. Elemental analyses were performed by Galbraith Laboratories, Microlytics, Dearfield Beach, MA; and the KSU University Anal. Lab.

Preparation of (η^6-toluene)bis(trifluorosilyl)nickel(II) (η^6-toluene)$Ni(SiF_3)_2$, (1, $X = F$) [45]*

To a 200 ml Schlenk tube, 0.42 g (1.0 mmol) of (η^6-toluene)$Ni(SiCl_3)_2$ (**1**) [16] dissolved in 50 ml of toluene was added through a fine filter frit. The Schlenk tube containing the resulting red brown solution was placed in a hood with good ventilation and was connected to the nitrogen gas line. Under N_2 flush and with rapid stirring 1.16 g (6.0 mmol) of $AgBF_4$ was added in small increments to the solution over a period of 20 min. After addition of the $AgBF_4$ the solution was stirred for 5 h. A vigorous reaction accompanied by BF_3 evolution, occurred during the addition of $AgBF_4$ to the solution. After 2 h BF_3 evolution began to decrease and after 4 h appeared negligible. Stirring was stopped after 5 h and the mixture filtered through a fine glass frit. Volatiles were stripped from the resulting yellow solution under vacuum leaving 0.250 g of yellow solid. The yield was 78.0% based on starting Ni complex. The spectroscopic data were the same as those obtained from authentic samples [42]. A ^{19}F NMR spectrum, taken in CD_2Cl_2, showed a single resonance 74.0 ppm downfield from hexafluorobenzene.

Preparation of bis(trichlorosilyl)tris(trimethylphosphine)nickel(II), $(Me_3P)_3Ni(SiCl_3)_2$

In the glove box, 0.42 g (1.0 mmole) of (η^6-toluene)$Ni(SiCl_3)_2$ dissolved in 30 ml of toluene, was added to a 200 ml Schlenk tube containing a magnetic stirring bar through a fine filter frit. The Schlenk tube, containing the resulting red brown solution, was removed from the glove box, frozen by liquid nitrogen and connected to a vacuum line. After one cycle of freeze/thaw degassing, 0.5 ml (about 7 mmol) of PMe_3 was added to the frozen solution by vacuum transfer. The mixture was allowed to warm slowly to room temperature and then stirred for 30 min. During this period a reaction occurred and the color of the solution changed from red brown to pale orange. The solvent was removed under vacuum. The residual orange solid was redissolved in pentane, filtered through a fine frit and the solvent then pumped off slowly. When the solvent was completely pumped off, 0.51 g of crystalline orange solid was left in the Schlenk tube. The yield was 92%. This solid was recrystallized from a minimum amount of pentane and the resulting pale orange crystals used for analysis.

$(PMe_3)_3Ni(SiCl_3)_2$: m.p. 115–120 °C. Analyses. Found: C, 19.67; H, 5.08; Cl, 38.36; P, 16.75. $C_9H_{27}NiP_3Si_2Cl_6$ calc.: C, 19.45; H, 4.85; Cl, 38.28; P, 16.72%. IR (Nujol/KBr, cm^{-1}) 470s, 670m, 710m, 730m, 790w, 860m, 870m, 945s, 960s, 1000–1200m, br, 1285m, 1310w, 1430w, sh, 1440m. Mass spectrum: 442(0.3) $M - PMe_3$, Cl; 345(1.5) $M - PMe_3$, $SiCl_3$; 210(100) $Ni(PMe_3)_2^+$; 134(35) Ni PMe_3^+; 76(20) PMe_3^+, 61(20) PMe_2^+. NMR see Table 1.

Preparation of bis(trifluorosilyl)tris(trimethylphosphine)nickel(II), $(Me_3P)_3Ni(SiF_3)_2$

The same procedure as described above was used, 0.32 g (1.0 mmol) of (η^6-toluene)$Ni(SiF_3)_2$ with 0.5 ml (7 mmol) of PMe_3 yielding a pale orange solid crystallized from pentane (0.42 g, 92%, m.p. 111–113 °C). Analyses. Found: C, 23.47; H, 6.04; P, 19.78. $C_9H_{27}NiP_3Si_2F_6$ calcd.: C, 23.65; H, 5.95; P, 20.33%. IR (Nujol/KBr, cm^{-1}) 470s, 670m, 720w, 730w, 780s, 820s, 830s, 860w, 870w, 950s, 960s, 1255w. Mass spectrum 455(3.0) M^+, 437(45) $M - F$, 361 (4.1) $M - PMe_3$, F; 286(21) $Ni(PMe_3)_3^+$, 209(7.6) $Ni(PMe_3)_2^+$, 76(100) PMe_3^+, 61(11) PMe_2^+. NMR see Table 1.

Preparation of bis(trichlorosilyl)tris(trimethylphosphite)nickel(II) $[(MeO)_3P]_3Ni(SiCl_3)_2$

In the glove box, 0.42 g (1.0 mmol) of (η^6-toluene)$Ni(SiCl_3)_2$ dissolved in 30 ml of toluene was added through a fine filter frit, to a 200 ml Schlenk tube containing a magnetic stirring bar. The Schlenk tube, containing the resulting red brown solution, was removed from the glove box and connected to a 60 ml addition funnel containing 0.4 ml (3.4 mmol) of $P(OMe)_3$ dissolved in 10 ml of toluene. The Schlenk tube was cooled to −30 °C by an isopropyl alcohol cold bath and the solution of $P(OMe)_3$ was added dropwise over a 10 min period. The resulting solution was stirred for 20 min. During this time a reaction occurred and the color of the solution changed from red brown to yellow. After 30 min the cold bath was removed and the volatiles stripped under vacuum leaving a yellow solid. This solid was redissolved in diethyl ether and the resulting yellow solution filtered through a fine filter frit. After the solvent was pumped off again 0.37 g of yellow solid was left in Schlenk tube. The yield was 51%, m.p. 101–105 °C, Analyses. Found: C, 16.76; H, 4.15; Cl, 29.09; P, 13.30. $C_9H_{27}O_9NiP_3Si_2Cl_6$ calcd.: C, 15.45; H, 3.86; Cl, 30.47; P, 13.41%. IR (Nujol mull, CsI plates) 475s, 550s, 728s, 780s, 1050s, br, 1175m, 1267w, 1590w cm^{-1}. Mass spectrum 133(6.0) $SiCl_3^+$, 124(25) $P(OMe)_3^+$, 93(100) $P(OMe)_2^+$, 62(28) $POMe^+$. NMR, see Table 1.

Preparation of bis(trifluorosilyl)tris(trimethylphosphite)nickel(II), $[(MeO)_3P]_3Ni(SiF_3)_2$

The procedure was similar to the above. Here 0.32 g (1.0 mmol) of (η^6-toluene)$Ni(SiF_3)_2$ was used. During addition of $P(OMe)_3$, the original yellow solution turned colorless. After stirring for 30 min, the volatiles were removed in-vacuo. During pumping the color of the solution gradually turned dark. When the volatiles were completely removed, some colorless solid, together with some black solid, was left in the Schlenk tube. This solid mixture was redissolved in pentane and the resulting gray solution was filtered through a fine filter frit. The nearly colorless filtrate was dried, leaving 0.34 g of colorless solid. The yield was 57%, m.p. 85–87 °C, Analyses Found: C, 18.12; H, 4.22; F, 18.47; P, 14.75. $C_9H_{27}O_9NiP_3Si_2F_6$ calcd.: C, 17.98; H, 4.52; F, 18.96; P, 15.46%. IR (Nujol/KBr, cm^{-1}) 470s, 480s, 550s, 720s, 790s, 850s, 1000-1100s, sh, 1180s, 1250s, 1630m, br. Mass spectrum 600(0.3) M^+, 569(1.4) $M-$ OMe, 430(20) $Ni[P(OMe)_3]_2^+$, 306(95) $Ni[P(OMe)_3]_2^+$, 182(43) $NiP(OMe)_3^+$, 124(21) $P(OMe)_3^+$, 93(100) $P(OMe)_2^+$, 62(24) $POMe^+$. NMR, see Table 1.

Preparation of bis(trichlorosilyl)tris(triethylphosphite)nickel(II), $[(EtO)_3P]_3Ni(SiCl_3)_2$

The procedure for this reaction was also similar to that given above. Here 0.63 ml (3.0 mmol) of $P(OEt)_3$ was used instead of $P(OMe)_3$. When the addition of $P(OEt)_3$ was complete the original red brown solution turned dark yellow. After stirring for 20 min the volatiles were pumped off leaving a black solid. This black solid was redissolved in diethyl ether and was filtered through a column (ID: 2.5 cm, length: 45 cm) packed with Florisil. The resulting filtrate was yellow. After the solvent was removed, 0.52 g of yellow solid was left in the Schlenk tube. The yield was 63%; m.p. 125–130 °C, IR (Nujol/KBr, cm^{-1}) 475s, 490s, sh, 556s, 718s, 765s, 805w, sh, 847s, 1030s, 1095w, 1150m, 1280w, br. NMR, see Table 1.

Preparation of bis(trifluorosilyl)tris(triethylphosphite)nickel(II), $[(EtO)_3P]_3Ni(SiF_3)_2$

The procedure for the reaction was similar to that above. Here, 0.63 ml (3.0 mmol) of $P(OEt)_3$ was used instead of $P(OMe)_3$. When the addition of $P(OEt)_3$ was complete the original yellow solution turned colorless. After stirring for 20 min the volatiles were pumped off leaving a white solid which was redissolved in pentane and filtered through a fine filter frit. After drying, the product was obtained as 0.54 g of colorless solid. The yield was 76%, m.p. 92–95 °C, Analyses Found: C, 29.81; H, 6.43; F, 15.17; P, 12.65. $C_{18}H_{45}O_9NiP_3Si_2F_6$ calcd.: C, 29.72; H, 6.23, F, 15.67; P, 12.77%. IR (Nujol/KBr, cm^{-1}) 460s, 550s, 715m, 780s, 850s, 945s, 1030s, 1095s, 1160m, 1250w, 1290w. NMR, see Table 1.

Preparation of bis(trichlorosilyl)bis(triethylphosphine)nickel(II), $(Et_3P)_2Ni(SiCl_3)_2$

The procedure was similar to that for $P(OMe)_3$ complexes. Here 0.45 ml (3.0 mmol) of PEt_3 was used instead of $P(OMe)_3$. When the addition was completed the color of the solution changed from red brown to dark orange. After stirring for 20 min the volatiles were removed in-vacuo leaving an orange purple solid. This solid was moderately soluble in pentane. By using a large amount of pentane it was redissolved and the pentane solution was filtered again. After the solvent was removed in-vacuo slowly 0.46 g of orange purple solid was left in the Schlenk tube. The yield was 82%, m.p. 107–110 °C, Analyses Found: C, 27.41;H, 5.89; P, 11.50. $C_{12}H_{30}NiP_2Si_2Cl_6$ calcd.: C, 25.55; H, 5.32; P, 11.00%. IR (Nujol/KBr, cm^{-1}) 470s, 670m, 710m, 730m, 790w, 860m, 870m, 945s, 960s, 1000–1200m, br, 1285m, 1310w, 1430w, sh, 1440m. Mass spectrum 249(6.6) $M-SiCl_3$, 364(13) $Ni(PEt_3)_2Cl_2^+$, 295(81) $Ni(PEt_3)_2^+$, 266(31) $NiP_2Et_5^+$, 134(75) $SiCl_3^+$, 98(15) $SiCl_2^+$, 90(66) PEt_2^+, 60(100) PEt^+. NMR, see Table 1.

Preparation of bis(2,6-lutidine)bis(trichlorosilyl)nickel(II), (Lut)$_2$Ni(SiCl$_3$)$_2$

To a solution of 1.0 g (9.3 mmol) 2,6-lutidine in 50 ml of CH_2Cl_2, 0.5 g (1.2 mmol) (η^6-toluene)Ni$(SiCl_3)_2$ was added, and the resulting solution stirred for 3 h, after which no further color change occurred. The solution was filtered and layered with 80–100 ml of pentane and stored at 0 °C for one week. Red crystals precipitated which were collected by decanting, washing with pentane, and drying in-vacuo; 80% yield. Analyses Found: C, 30.84; H, 3.35; N, 5.08. $C_{14}H_{18}N_2NiSi_2Cl_6$ calcd.: C, 31.03; H, 3.32; N, 5.17%. IR (nujol mull and CsI plates) 470vs, 510vs, 540vs, 732m, 775s, 782s, 900w, 1020m, 1030m, 1110m, 1165s, 1250w, 1395m, 1575s, 1603s, 1640w cm^{-1}. Mass spectrum (95 °C, 18 eV, EI) 268(0.3) $Si_2Cl_6^+$, 206(0.1) $C_7H_9NSiCl_2^+$, 170(13) $C_7H_9NSiCl^+$, 135(20) $C_7H_9NSi^+$, 132(21) $SiCl_3^+$, 107(100) $C_7H_9N^+$. NMR, see Table 1.

Preparation of bis(2,4,6-collidine)bis(trichlorosilyl)nickel(II), (coll)$_2$Ni(SiCl$_3$)$_2$

To a solution of 1.1 g (9.1 mmol) 2,4,6-collidine in 50 ml of CH_2Cl_2, 0.5 g (1.2 mmol) of (η^6-toluene)Ni$(SiCl_3)_2$ was added, and the resulting solution stirred for 3 h, after which the color changed from red to burgundy. The solution was filtered and layered with 100 ml of pentane and kept at 0 °C for one week. Large cube shaped bright red crystals formed were collected by decantation and dried in-vacuo. The yield was 95%. If exposed to air the crystals turn greenish on the surface. Analyses Found: C, 33.76; H, 4.11, N, 4.96; Ni, 9.97. $C_{16}H_{22}N_2NiSi_2Cl_6$ calcd.: C, 33.72; H, 3.86; N, 4.92, Ni, 10.36%. IR (fluorolube mull and CsI plates) 470vs, 490vs, 510vs, 535vs, 725m, 800m, b, 845m, 858m, 935w, 1020m, br, 1260w, 1310w, 1402w, 1550m, br, 1610s cm^{-1}. Mass spectrum (131 °C, 19 eV, EI) 170(2.7) $C_8H_{11}NSiCl^+$, 149(6.2) $C_8H_{11}NSi^+$, 132(3.3) $SiCl_3^+$, 121(100) $C_8H_{11}N^+$. NMR, see Table 1.

Preparation of tri(pyridine)bis(trichlorosilyl)nickel(II), (py)$_3$Ni(SiCl$_3$)$_2$

To a solution of 1.00 g (12.6 mmol) of pyridine in 50 ml of CH_2Cl_2, 0.5 g (1.2 mmol) of (η^6-toluene)Ni$(SiCl_3)_2$ was added, and the resulting solution stirred for 3 h after which the color changed from red to light brown. The solution was filtered and the solvent removed in-vacuo leaving an orange oil along with some white solid. This residue was redissolved in 200 ml THF. 50 ml of diethyl ether was added and the resulting yellow solution cooled to −10 °C for several days. The white material separated, was filtered off and discarded. The solvent was removed from the remaining yellow solution, leaving a yellow oil which slowly solidified. Analyses Found: C, 32.73; H, 3.02; N, 7.40. $C_{10}H_{10}N_2NiSi_2Cl_6$ calcd.: C, 31.90; H, 2.66; N, 7.44%. IR (fluorolube mull and CsI plates) 1440m, 1450m, 1480m, 1595w, 1610m, 1625w, 2550w, 2910w, 2980w cm^{-1}. Mass spectrum (126 °C, 35 eV, EI) 212(42) $C_5H_5NSiCl_3^+$, 177(3.0) $C_5H_5NSiCl_2^+$, 142(11) $C_5H_5NSiCl^+$, 132(52) $SiCl_3^+$, 79(100) $C_5H_5N^+$. NMR, see Table 1.

Preparation of bis(2,4,6-collidine)bis(acetato)copper(II), (coll)$_2$Cu(O$_2$CCH$_3$)$_2$

In order to obtain IR spectra this material was prepared as described earlier [32] and recrystallized from ethanol/acetic acid.

Reaction of [(MeO)$_3$P]$_3$Ni(SiCl$_3$)$_2$ with NaCo(CO)$_4$. Preparation of [(MeO)$_3$P]$_2$Ni(SiCl$_3$)$_2$(CO)

Two grams (2.86 mmol) of the phosphite complex was slurried in 200 ml of cyclohexane and 1.0 g (6.0 mmol) of NaCo(CO)$_4$ was added in one batch to the stirred mixture. After 10 min the mixture changed from colorless to red. Stirring was continued for 48 h and the mixture turned brown. Removal of solvent in-vacuo left a brown solid which was continuously extracted with 300 ml of pentane, and then 200 ml of diethyl ether. Both extracts were filtered and concentrated to half their volumes. Cooling to −10 °C for several days produced light yellow crystals from the ether extract and large red crystals and white material from the pentane extract. Mechanical separation of the white and red crystals, in the glove box, and two recrystallizations of each material yielded pure samples of $[(MeO)_3P]_2Ni(SiCl_3)_2CO$ and $[(MeO)_3P]_2Co_2(CO)_6$ as pure samples (about 50% yields). For $[(MeO_3P]_2$-$Ni(SiCl_3)_2CO$. Analyses Found C, 14.25; H, 3.13; Cl, 36.00; Ni, 9.53; P, 10.00; Si, 8.99. $C_7H_{18}O_7NiP_2Si_2Cl_6$ calcd.: C, 13.92; H, 2.98; Cl, 35.30; Ni, 9.71; P, 10.25; Si, 9.29%. IR (Nujol mull, CsI plates) 495s, 530s, 545s, 560m, 770s, 800s, 830s, 1040s, 1070s, 1090s, 1995w, 2060s cm^{-1}. Mass spectrum MS (50 °C, 20 eV, EI) 134(38) $SiCl_3^+$, 92(100) $POMe^+$, 109(50) $P(OMe)_2^+$, 124(94) $P(OMe)_3^+$. NMR, see Table 1. For $[(MeO)_3P]_2Co_2(CO)_6$. Analyses Found: C, 27.13; H, 3.51; Co, 20.58. $C_{12}H_{18}O_{12}$ Co_2P_2 calcd.: C, 26.90; H, 3.37; Co, 22.06%.

Preparation of tris(trifluorophosphine)bis(trichlorosilyl)nickel(II), $(F_3P)_3Ni(SiCl_3)_2$

$(\eta^6$-Toluene)$Ni(SiCl_3)_2$ (2.0 g, 4.8 mmol) was dissolved in 100 ml of $C_6H_5CF_3$ resulting in a deep red solution ($C_6H_5CF_3$ does not coordinate to the $Ni(SiCl_3)_2$ moiety). After three freeze-pump-thaw degassing cycles the flask was filled with PF_3 gas and PF_3 was bubbled through the solution, with stirring. After 2–3 minutes the color turned from deep red to yellowish white, and a small amount of black precipitate formed. The solution was filtered and the solvent removed in-vacuo leaving 1.2 g (2.0 mmol, 42% yield) of $(F_3P)_3Ni(SiCl_3)_2$ as a greyish-white powder. The product is sensitive and decomposed in THF, diethyl ether, and pentane at room temperature. An analytically pure sample was obtained by washing at −20 °C with cold hexane, and subliming at 35 °C (10^{-3} Torr) in a long glass tube. Analyses. Found: Ni, 9.08; P, 14.70; Si, 8.83. $P_3NiSi_2Cl_6F_9$ calcd.: Ni, 9.91; P, 15.70; Si, 9.49%. IR (nujol mull, CsI salt plates) 325w, 390s, 480s, 505s, 562s, 875s, 910s, 920s. Mass spectrum (30 °C, 18.1 eV, CI using CH_4) 466(100) $Ni(SiCl_2)(SiCl_3)(PF_3)_2^+$, 378(67)$Ni(SiCl_2)(SiCl_3)(PF_3)^+$, 269(4) $Si_2Cl_6^+$, 157(19) $NiSiCl_2^+$, 132(8) $SiCl_3^+$, 88(82) PF_3^+ (expected isotope patterns for Cl and Ni were obtained). ^{19}F NMR, see Table 1.

A similar reaction with $(\eta^6$-toluene)$Ni(SiF_3)$ gave no reaction.

Reaction of $(\eta^6$-benzene)$Ni(SiCl_3)_2$ with PCl_3. Preparation of $Ni(PCl_3)_4$

$(\eta^6$-Toluene)$Ni(SiCl_3)_2$ (1.0g, 2.8 mmol) was exchanged two times with benzene as described earlier [17b,46]. The resulting $(\eta^6$-benzene)$Ni(SiCl_3)_2$ was dried in vacuo and 2.0 g (15 mmol) of PCl_3 distilled in under vacuum while the flask was cooled in liquid nitrogen. The mixture was warmed and stirred for 5 min at room temperature. Addition of 20 ml pentane, filtration of the resulting solution (now colorless) followed by cooling to −20 °C yielded $Ni(PCl_3)_4$ as white crystals (47%) yield) [47]. Analyses. Found: Cl, 71.93; P, 20.58. P_4NiCl_{12} calcd.: Cl, 69.90; P, 20.40%. IR (Nujol mull) 325s, 500s, 570s, 805m, 870m cm^{-1}.

X-Ray structure determination of bis(2,4,6-collidine)bis(trichlorosilyl)nickel(II)

A red wine colored crystal of the compound was wedged inside a thin walled glass capillary with brief exposure to air. The unit cell was examined and data collected on a Picker Diffractometer automated with a Crystal Logic control system [48*]. Lattice constants were verified by axial photographs. The count rate for 8 of the scanned reflections (012, 020, 100, 106, 112, 142, 20-4, and 20-2) exceeded the maximum allowed count rate of 50000 cps and, consequently, could not be processed). A summary of crystal data is given in Table 5. The intensity of 3 standard reflections decreased by 4.7% over the 121.2 h of exposure time which was used as a basis for a decay correction that was applied to the data set. The position of the Ni atom was located from a Patterson synthesis. Fourier syntheses were used to locate the remaining non-hydrogen atoms. The structure was refined isotropically to an R value of 10.4% followed by fully anisotropic refinement, with the inclusion of the 4 aromatic hydrogen atoms at theoretical positions as fixed contributors, which produced an R value of 3.9%. A difference synthesis at this stage revealed regions of electron density for these methyl hydrogens were then calculated in these regions, at a distance of 1.0 Å, and included in final refinement as fixed contributors. Absorption corrections were added in the final refinement which converged with an R of 3.1% and a weighted R_w of 4.2%.

Supplementary material available. Listings of anisotropic thermal parameters (Table 8, 2 pages) and structure factor amplitudes (Table 9, 15 pages) are available. Ordering information is given on any current masthead page.

Acknowledgements

The support of the National Science Foundation is acknowledged with gratitude. JJS thanks the Fulbright Commission for a travel grant and the Fonds der Chemischen Industrie for partial financial support.

References

1 F. Hein, H. Pobloth, Z. Anorg. Allg. Chem., 248 (1941) 84.
2 T.S. Piper, D. Lemal, G. Wilkinson, Naturwissenschaften, 43 (1956) 129.
3 B.J. Aylett, J.M. Campbell, J. Chem. Soc., Chem. Commun., (1965) 217.
4 A.J. Chalk, J.F. Harrod, J. Am. Chem. Soc., 87 (1965) 1133.
5 F. Glockling, A. McGregor, M.L. Schneider, H.M.M. Shearer, J. Inorg. Nucl. Chem., 32 (1970) 3101.
6 F. Glockling, A. McGregor, J. Inorg. Nucl. Chem., 35 (1973) 1481.
7 C.W. Cheng, C.S. Liu, J. Chem. Soc., Chem. Commun., (1974) 1013.
8 T. Kruck, E. Job, U. Klose, Angew. Chem., Int. Ed. Engl., 7 (1968) 374.
9 M.F. Lappert, G. Speier, J. Organomet. Chem., 80 (1974) 329.
10 C.S. Liu, C.W. Cheng, J. Am. Chem. Soc., 97 (1975) 6746.
11 E. Uhling, B. Hipler, P. Muller, Z. Anorg. Allg. Chem., 442 (1978) 11.
12 N.S. Biradar, V.L. Roddabasanagoudar, T.M. Aminabhavi, Polyhedron, 3 (1984) 603.
13 Y. Kiso, K. Tamao, M. Kumada, J. Organomet. Chem., 76 (1974) 105.
14 (a) W. Jetz, W.A.G. Graham, J. Am. Chem. Soc., 89 (1967) 2773; (b) S.T. Lin, T.J. Groshens, K.J. Klabunde, Inorg. Chem., 23 (1984) 1.
15 T. Groshens, K.J. Klabunde, Organometallics, 1 (1982) 564.
16 S.T. Lin, R.N. Narske, K.J. Klabunde, Organometallics, 4 (1985) 571; S.B. Choe, K.J. Klabunde, Organomet. Synth., 3 (1986) 156.
17 (a) H. Kanai, S.B. Choe, K.J. Klabunde, J. Am. Chem. Soc., 108 (1986) 2019; (b) S.K. Janikowski, L.J. Radonovich, T.J. Groshens, K.J. Klabunde, Organometallics, 4 (1985) 396.
18 (a) H.F. Klein, Angew. Chem. Int. Ed. Engl., 19 (1980) 362; (b) T.R. Bierschenk, M.A. Guerra, T.J. Juhlke, S.B. Larson, R.J. Lagow, J. Am. Chem. Soc., 109 (1987) 4855.
19 P.W. Jolly, in G. Wilkinson, F.G.A. Stone, E.W. Abel, (Eds.), Comprehensive Organometallic Chemistry, Vol. 6, p. 37, Pergamon Press, New York, N.Y. 1982.

20 C.A. Tolman, J. Am. Chem. Soc., 92 (1970) 2956.

21 Both $NiI_2(Coll)_2$ and $NiBr_2$ (2,6-Lut)$_2$ are tetrahedral and paramagnetic; see J.R. Allan, D.H. Brown, R.H. Nutall, D.W. Sharp, J. Inorg. Nucl. Chem., 27 (1965) 1305. For a detailed discussion of stereochemistry and magnetic properties of tetrahedral Ni^{II} derivatives, see J.R. Miller, Adv. Inorg. Radiochem., 4 (1962) 133; and R.S. Nyholm, Chem. Rev., 53 (1953) 266.

22 See e.g. the review by K.H. Panell, B.L. Kalsotra, C. Parkanyi, J. Heterocyc. Chem., 15 (1978) 1057.

23 J. Buckingham (Ed.), Dictionary of Organometallic Compounds, Vol. II, Nickel, Chapman and Hall, London, 1984.

24 P.W. Jolly, in G. Wilkinson, E.W. Abel, F.G.A. Stone (Eds.), Comprehensive Organomet. Chemistry," Vol. VI, Nickel, Pergamon Press, New York, 1982.

25 J.M. Coronas, C. Polo, J. Sales, Inorg. Chim. Acta, 48 (1981) 87.

26 M. Wada, K. Ogura, Y. Kawasaki, J. Organomet. Chem., 178 (1979) 261, and ref. cited therein.

27 (a) L.H. Simons, P.E. Riley, R.E. Davis, J.J. Lagowski, J. Am. Chem. Soc., 98 (1976) 1044; (b) P.E. Riley, R.E. Davis, Inorg. Chem., 15 (1976) 2735; (c) J. Koch, Ph.D. Dissertation, Philipps Universitaet Marburg, W. Germany, 1981; (d) E.J. Wucherer, E.L. Muetterties, Organometallics, 6 (1987) 1691; (e) J. Kroker, Ph.D. Dissertation, Philipps Universital, Marburg, West Germany, 1986; (f) H.G. Biedermann, K. Ofele, J. Tajtelbaum, Z. Naturf. B, 31 (1976) 321; (g) H.G. Biedermann, K. Ofele, N. Schuhbauer, J. Tajtelbaum, Angew. Chem. Int. Ed. Engl., 14 (1975) 639.

28 A. Arcas, P. Royo, Inorg. Chim. Acta, 31 (1978) 97.

29 J.M. Coronas, G. Muller, M. Rocamora, J. Sales, J. Organomet. Chem., 184 (1980) 263.

30 R.G. Miller, R.D. Stauffer, D.R. Fahey, D.R. Parnell, J. Am. Chem. Soc., 92 (1970) 1511.

31 M. Pfeffer, P. Braunstein, J. Dehand, Spectrochim. Acta, A, 30 (1974) 331.

32 A. Busnot, F. Busnot, A. Leclaire, M. Bernard, Z. Anorg. Allg. Chem., 503 (1983) 207.

33 M.M. Brezinski, J. Schneider, L.J. Radonovich, K.J. Klabunde, Inorg. Chem., 28 (1989) 2414.

34 W.R. Busing, K.D. Martin, H.A. Levy, Report ORNL-TM-306; Oak Ridge National Laboratory: Oak Ridge, TN, 1964.

35 K.M. Mackay, B.K. Nicholson, in G. Wilkinson, F.G.A. Stone; E.W. Abel, (Eds.), Comprehensive Organometallic Chemistry, Vol. 9, p. 1043, Pergamon Press Ocford, 1982; E.H. Brooks, R.J. Cross, Organomet. Chem., Rev. A, 6 (1970) 227.

36 W. Malisch, J. Organomet. Chem., 82 (1974) 185.

37 W. Malisch, W. Kuhn, Chem. Ber., 107 (1974) 979.

38 C. Saint-Jolly, M. Dartiguenare, Y. Dartiguenare, Adv. Chem. Ser., 173 (1979) 152.

39 P.W. Jolly, in G. Wilkinson, F.G.A. Stone, E.W. Abel (Eds.), Comprehensive Organometallic Chemistry, Vol. 6, Nickel, Pergamon Press, Oxford.

40 Th. Kruck, Angew. Chem. Int. Ed., 6 (1967) 53.

41 V. Mark, C.H. Durgan, M.M. Crutchfield, J.R. Van Wazer, Top. Phosphorous Chem., 15 (1967) 227.

42 S.T. Lin, T. Groshens, K.J. Klabunde, Inorg. Chem., 23 (1984) 1.

43 R.J. Lagow, J.L. Margrave, Prog. Inorg. Chem., 26 (1979) 161–210.

44 W.F. Edgell, J. Lyford, IV, Inorg. Chem., 9 (1970) 1932.

45 S.B. Choe, K.J. Klabunde, Organometallic Syn., 3 (1983) 156 reports this fluorination procedure. The procedure reported herein is further modified and improved.

46 T.J. Groshens, K.J. Klabunde, J. Organomet. Chem., 259 (1983) 337.

47 J.W. Irvine, G. Wilkinson, Science, 113 (1951) 742.

48 The programs used in this structure determination were supplied by Crystal Logic. The Crystal Logic package includes modified versions of the following programs: REDUCE (Broach, Coppens, Becker and Blessing), peak profile analysis, Lorentz and polarization corrections; MULTAN (Main), package of programs, including direct methods, structure factor normalization, Fourier transform, and peak search; ORFLS (Busing Martin and Levy), structure factor calculation and full matrix least-squares refinement; ORFFE (Busing, Martin, and Levy), distance, angle, and error calculations; ABSROB (Coppens, Edwards and Hamilton), absorption correction calculation; ORTEP (Johnson) figure plotting; HYDROGEN (Trueblood), calculation of hydrogen atomic positions. All calculations were performed on a DEC MicroVax II computer. Scattering factors and corrections for anomalous dispersion were taken from: "International Tables for X-ray Crystallography"; Kynoch Press: Birmingham, England, 1974, vol. IV. $R = (\Sigma|F_o - F_c|/\Sigma|F_o|)$; $R_w = (\Sigma w|F_o - F_c|^2/\Sigma w|F_o|^2)^{1/2}$, where F_o and F_c are observed and calculated structure factors, respectively, and $w = 1/\sigma^2(F_o)$.